



Article

Phosphorylation but Not Oligomerization Drives the Accumulation of Tau with Nucleoporin Nup98

Lisa Diez ¹, Larisa E. Kapinos ², Janine Hochmair ¹, Sabrina Huebschmann ¹, Alvaro Dominguez-Baquero ¹, Amelie Vogt ¹, Marija Rankovic ³, Markus Zweckstetter ^{3,4}, Roderick Y. H. Lim ² and Susanne Wegmann ^{1,*}

Supplemental information

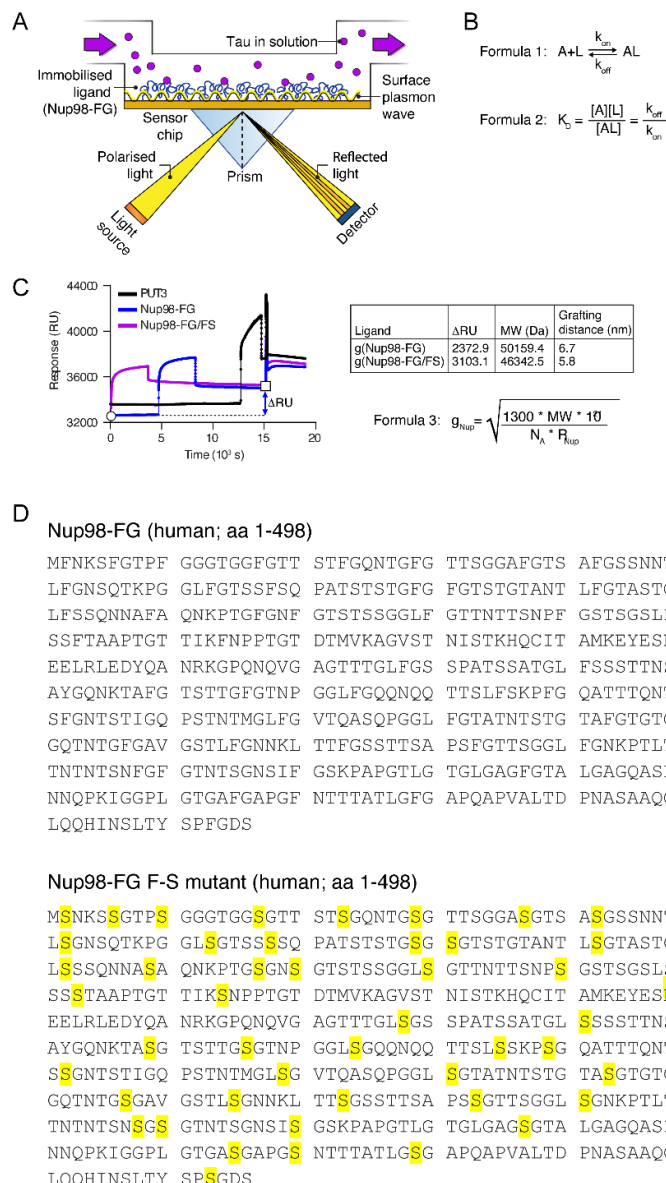


Figure S1. SPR principle, binding kinetics, and Nup98-FG layer immobilization. (A) Scheme of SPR experimental setup. The SPR sensor detects the binding of an analyte (e.g. Tau) in solution to a ligand (e.g. Nup98-FG) immobilized on the gold surface of the sensor chip. This binding alters the refractive index of the medium near the surface, which is monitored by a detector. (B) Formula 1

and Formula 2 for binding kinetics. (C) Immobilization of gold sensor chip for experiment shown in Figure 1F. In the shown example, the grafting distance, which gives information on how spares/dense the Nup98-FG layer is packed, is similar for the analyzed Nup98 variants (Nup98-FG and Nup98-FG/FS mutant). The grafting distance g (Nup98-FG) is calculated using the indicated formula with NA being the Avogadro constant, MW the molecular weight of Nup98-FG, and ΔRU the difference in SPR response before (white circle, $t = 0$ s) and after (white square, $t = 15 \times 10^3$ s) Nup98-FG immobilization. ΔRU of 1300 equals 1 ng Nup98-FG/mm² sensor chip surface. (D) Peptide sequence of Nup98-FG and Nup98-FG F/S mutant.

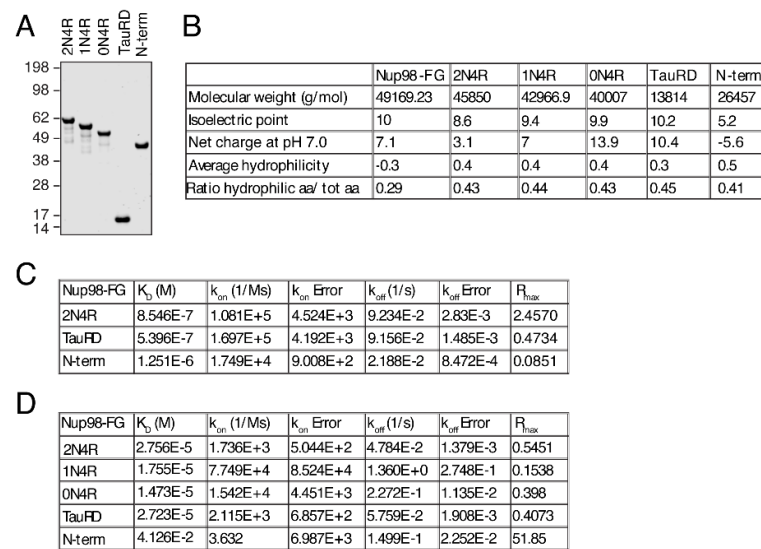


Figure S2. Biochemical and binding kinetic data for Tau variants. (A) Coomassie gel of recombinant expressed Tau variants. (B) Protein biochemical properties of Tau variants. (C) Association (k_{on}) and dissociation constants (k_{off}) for Tau 2N4R, TauRD, and N-term binding to Nup98-FG. Values derived from fits to the data shown in Figure 2D. (D) Association (k_{on}) and dissociation constants (k_{off}) for Tau isoform and domain binding to Nup98-FG. Values derived from fits to the data shown in Figure 2F.

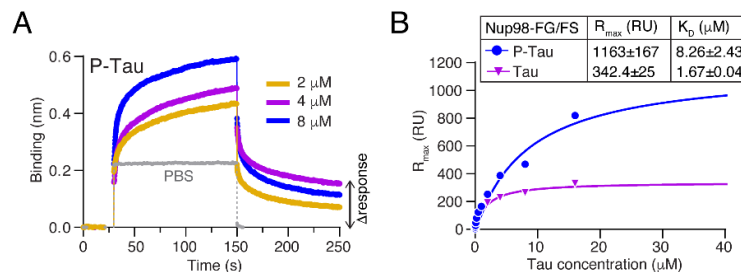


Figure S3. Binding kinetics of P-Tau to Nup98-FG/FS. (A) BLI measurement of P-Tau (2, 4 and 8 μ M) binding to Nup98-FG compared to PBS (grey). The accumulation of P-Tau on the Nup98-FG layer is apparent from the incomplete dissociation (Δ response). (B) Equilibrium fit (Langmuir binding isotherm) to RU_{max} plotted versus Tau concentration for the binding of Tau and P-Tau to mutant Nup98-FG/FS. In the Table, fit results are shown as value±SD.

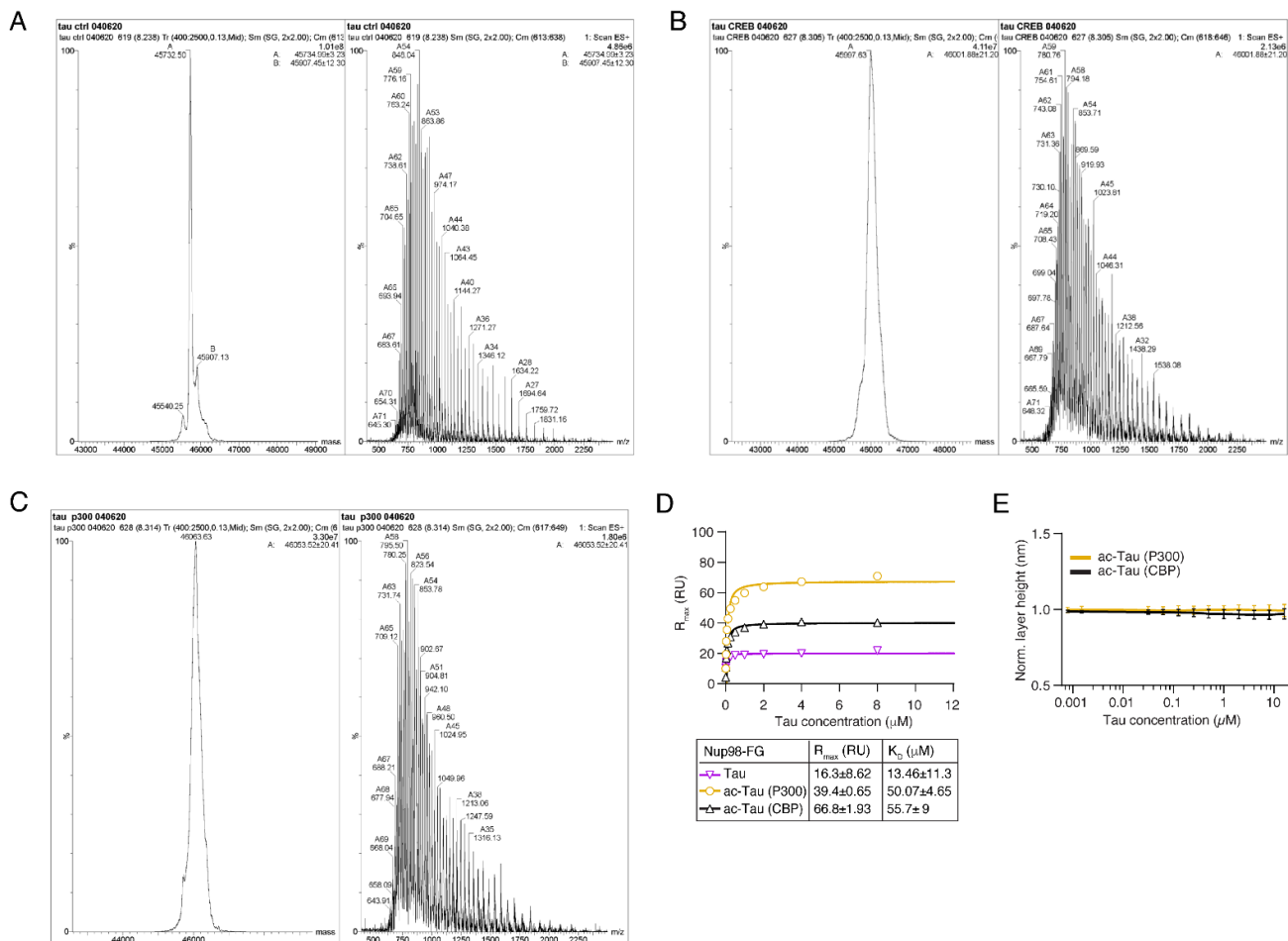


Figure S4. Mass spectrometry analysis of Tau acetylation and binding kinetics of ac-Tau to Nup98-FG. (A-C) Mass spectra of unmodified (A), CBP acetylated (B) and P300 acetylated Tau (C). Identified masses (in Da) are indicated showing Tau acetylation at 6-8 sites. (D) Equilibrium fit (Langmuir binding isotherm) to RU_{max} (from SPR measurements) plotted *versus* Tau concentration for the binding reactions of acetylated Tau compared to unmodified Tau. Tau was acetylated *in vitro* using P300 or CBP. In the Table, fit results are shown as value±SD. (E) Layer height analysis of *in vitro* acetylated Tau (using P300 or CBP) shows no accumulation of Tau on the Nup98-FG layer.

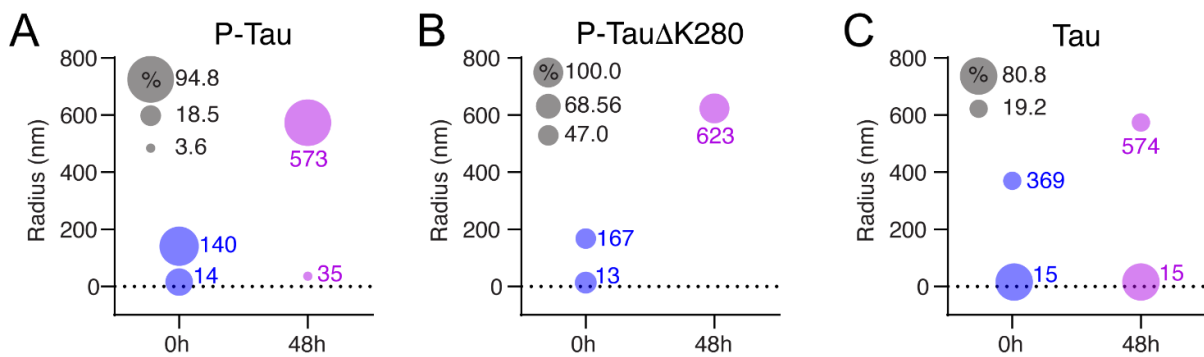


Figure S5. Radii of Tau measured by DLS before (0h) and after (48h) oligomerization. (A-C) Bubble plots of particle sizes for P-Tau (A), P-Tau Δ K280 (B) and Tau (C) before (0 h, blue) and after (48 h, purple) incubation at room temperature to enable oligomerization. Bubble sizes correspond to the %-age of different radius populations present (same data as shown in Figure 4A), and numbers in bubbles indicate the mean radius in nm.. The majority of P-Tau and P-Tau Δ K280 particles have a larger radius after 48h, indicating their oligomerization. Most Tau particles remain small, indicating a monomeric state.